EVALUATION OF CROSS SECTION PROCESSING CODES COMBINE AND WIMS FOR PEBBLE BED REACTOR FUEL CYCLE ANALYSIS

Steven E. Keller, Farzad Rahnema
Georgia Institute of Technology
School of Mechanical Engineering
Atlanta, GA 30332-0405, USA
sekeller1@yahoo.com, farzad.rahnema@me.gatech.edu

Cassiano de Oliveira, Matthew D. Eaton
Department of Earth Science and Engineering
Imperial College of Science, Technology and Medicine
Prince Consort Rd, London SW7 2BP, UK
c.oliveira@ic.ac.uk, m.eaton@ic.ac.uk

Abderrafi M. Ougouag, Hans D. Gougar, and William K. Terry
Idaho National Engineering and Environmental Laboratory
P.O. Box 1625
Idaho Falls, ID 83415-3885, USA
oom@inel.gov, goughd@inel.gov, wkt@inel.gov

ABSTRACT

Several transport and cross section processing code systems were evaluated for the production of three-dimensional cell-averaged cross sections for pebble-bed reactor (PBR) fuel cycle analysis. Comparisons of the multiplication factor, reaction rates and computation times based on calculations from the TORT discrete ordinates, the EVENT spherical harmonics, and the MCNP Monte Carlo codes were made, as well as between the COMBINE and WIMS cross section processing codes. Comparisons were also made between TORT models using various levels of quadrature and orders of Legendre expansion of the scattering cross sections.

An MCNP model with continuous-energy cross sections was used as the benchmark against which the MCNP, TORT, and EVENT models, all using 75-group cross sections produced by COMBINE calculations, were compared. Additionally, an EVENT model using 75-group and 172-group cross sections produced using WIMS was compared to the MCNP continuous-energy model.

It is found that COMBINE is not suitable as a cross section generator for PBR fuel cycle analysis. The WIMS code produces more accurate results than COMBINE, but results of reaction rate calculations not currently available need to be evaluated before its suitability for PBR cross section development can be fully determined.

1. INTRODUCTION

The objective of this work was to evaluate transport codes and cross section generation codes for the purpose of generating cross sections for pebble-bed reactors (PBRs). The cross sections will be used in the PBR fuel cycle analysis code PEBBED [1] at the Idaho National Engineering and Environmental Laboratory (INEEL). The cross section generation method would use a transport code with a fine-group (e.g., a 75-group) cross section library to calculate a flux spectrum, which would then be used to collapse and homogenize cross sections over a three-dimensional pebble cell to between 2 and 4 coarse groups.

Initially, the COMBINE cross-section processor and the TORT discrete ordinates transport code were used for this purpose. However, several problems were observed when using these two codes. TORT uses excessive computation time when compared to the EVENT code. Also, the modeling of the fuel pebble cell in three-dimensional geometry (e.g., spherical pebble inside a cube of gas) by TORT is substantially more complicated and time consuming than it is by EVENT. Seventy-five-group cross sections produced by COMBINE and used in MCNP show large differences in the multiplication factor when compared to the same MCNP model using continuous-energy cross sections. Because of these problems, the EVENT transport code and WIMS cross section processing codes were also evaluated for possible use.

2. MODEL DESCRIPTIONS

2.1 ACTUAL PBR PEBBLE

The PBR pebble consists of a spherical fuel region 2.5 cm in radius containing between 9000 and 25000 coated fuel particles (1 mm o.d.) in a graphite matrix. A graphite shell 0.5 cm thick surrounds the fuel region of the pebble. The pebbles rest at the bottom of the reactor core with a packing fraction of between 61 and 64%. Helium coolant is forced to flow downward in the core. The mean pebble temperature during operation is approximately 1000˚ C. Graphite at 1000 K was used for the operating temperature calculations, and graphite at 300 K was used for the cold temperature calculations.

Since the arrangement of the pebbles resting in the core is random, cubic pebble models, such as the one shown in Fig. 1, introduce an inaccuracy by the non-random repetitive arrangement of the pebbles in the model. Despite this inaccuracy, cubic arrangements were considered for simplicity. The simple cubic cell shown in Fig. 1, with 1/8 of a pebble at each corner, and with the edges of the pebbles touching each other, would provide a maximum packing fraction of only 52%. The space between the pebbles represents He coolant. The body centered cubic (BCC) cell shown in Fig. 2, however, can have a packing fraction of up to 66 %, depending on the pitch chosen. This makes the BCC cell a better choice than the simple cubic cell for modeling the PBR.

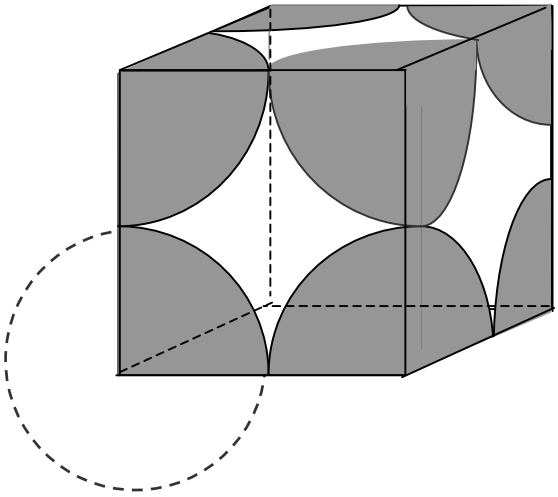

Figure 1. Simple cubic cell.

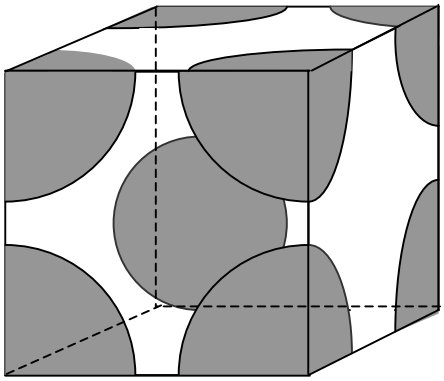

Figure 2. Body centered cubic cell.

While the BCC cell has a packing fraction that is closer to that of an actual PBR, it is believed that the simple cubic (SC) cell model is adequate for the purpose of evaluating the cross section processing methodology. Therefore, the pebble cell modeled in the transport calculations in this project is either a single pebble in a cube of gas, shown in Fig. 3, or an octant of this single pebble cell. Which version of this cell was modeled is explained below in the respective TORT, EVENT, and MCNP model descriptions. A 2-dimensional cross-section cut of this single pebble cell is shown in Fig. 4. The pebble in the single pebble cell has a fuel region with a 2.5-cm radius, and is composed of the fuel particles and graphite matrix homogeneously mixed throughout the region. It is surrounded by a 0.5-cm-thick graphite shell. The sides $\boldsymbol{l}$ of the cube are 6.2 cm long.

3. PEBBLE MODELS

3.1 COMBINE [2]

The COMBINE-PC version 5.23 (February 1990) was used in this study. This code solves the B-1 or B-3 approximation to the Boltzmann transport equation in one dimension for a homogeneous bare slab. The homogeneous region included all of the materials in the fuel particles, carbon matrix, graphite shell, and surrounding coolant. Spherical geometry was specified for the thermal disadvantage factor calculation, for which COMBINE uses the ABH [3] method. A homogenized fuel region with a 2.5-cm radius, a graphite shell region with a 3-cm radius, and a coolant region with a 3.509-cm radius were used as input for the ABH calculation. A Dancoff-Ginsburg factor of 0.312 was used to account for the neighboring pebbles [4], but none was used to account for the fuel particle heterogeneity. The cross sections were from the ENDF/B-V library. All COMBINE cross sections in this paper use a 75-group structure.

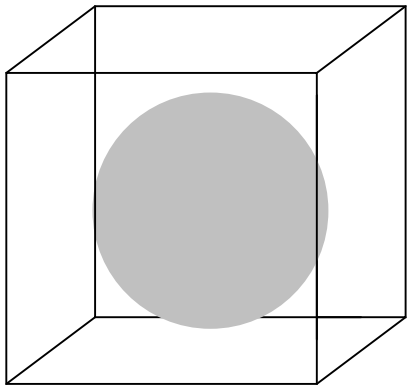

Figure 3. Single pebble cell.

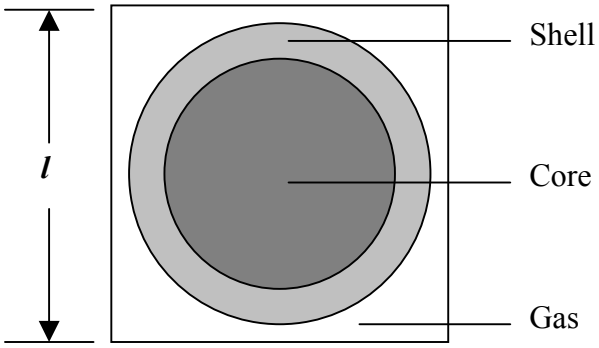

Figure 4. Cross-sectional view of single pebble cell.

3.2 WIMS [5]

WIMS version 8A (May 1999) was used in this study. A 75-group cross section library was generated from the 172-group master library cross sections. The 75-group cross sections used the same energy structure that was used in COMBINE. The WIMS cell model geometry is infinite cylindrical geometry with corrections made for the different mean chord length of cylindrical

geometry compared to spherical geometry. A Dancoff factor of 0.312 was used to account for surrounding pebbles. The Dancoff factor is a function of the mean chord length in the pebble. Spherical-geometry characteristic calculations were performed using the cross sections obtained from the WTHESEUS [5]-generated collision probability self-shielded cross sections. These calculations with the characteristic method replicate the EVENT 1D model exactly (although with a different discretization scheme) including white albedo. The results are in close agreement with the EVENT runs. The WIMS model used the JEF2.2 library with 172 groups.

3.3 TORT [6]

TORT version 3 (October 1997) supplied within the DOORS3.2 package was used in this study. TORT uses cylindrical or rectangular geometry. Rectangular geometry was chosen to model the single pebble cell. A 6.2-cm cube-shaped region was divided into 42 evenly spaced intervals in the x, y, and z directions. The result was 74088 fine mesh cells, each one measuring approximately 0.15 cm per side. Each one of the fine mesh cells was assigned one of three materials, fuel, shell, or gas. The material compositions of the fine mesh cells were chosen so that two concentric spherical regions would result, one modeling the fuel region and one modeling the shell region, all contained inside a gas cube. A cross-sectional view of the TORT model is shown in Fig. 5. One plane of fine mesh cells is visible, as are the fuel, graphite shell, and surrounding gas regions. There are 20072 mesh cells representing the fuel region, 13040 mesh cells representing the shell region, and 40976 representing the surrounding gas region.

The volume of fuel has been conserved between the single pebble cell and the TORT model. However, it was not possible to conserve the graphite shell volume in the TORT model. This occurred because in order to maintain the best approximation possible to a spherically shaped shell using the cube-shaped mesh cells, the resulting shell volume was 10.8% too small. For this reason, the density of the graphite shell region was multiplied by the ratio of the shell volume in the single pebble cell to that in the TORT model. This modification to the TORT model conserved the number of atoms in the graphite shell region.

The volume of the gas region surrounding the pebble was conserved in the TORT model. In order to do this the length of the side of the gas cube region containing the pebble had to be reduced from 6.2 cm to 6.15 cm. Specular reflective boundary conditions were used on all sides of the cube.

3.4 EVENT [7]

EVENT version v3.3ar3 (February 2002) was used in the calculations. EVENT uses a mesh generator to generate an accurate 3-dimensional finite element model of the two-region spherical

pebble in a gas cube. Only an octant needs to be modeled because of existing symmetry. The mesh consisted of 160 nodes and 247 hexahedral elements. A P_3 angular approximation and P_1 scattering expansion were used.

3.5 MCNP [8]

The version of MCNP used is MCNP4B (February 1997). In the MCNP model, the pebble was modeled exactly as two concentric spheres representing the fuel and shell regions, in a cube of gas 6.2 cm per side.

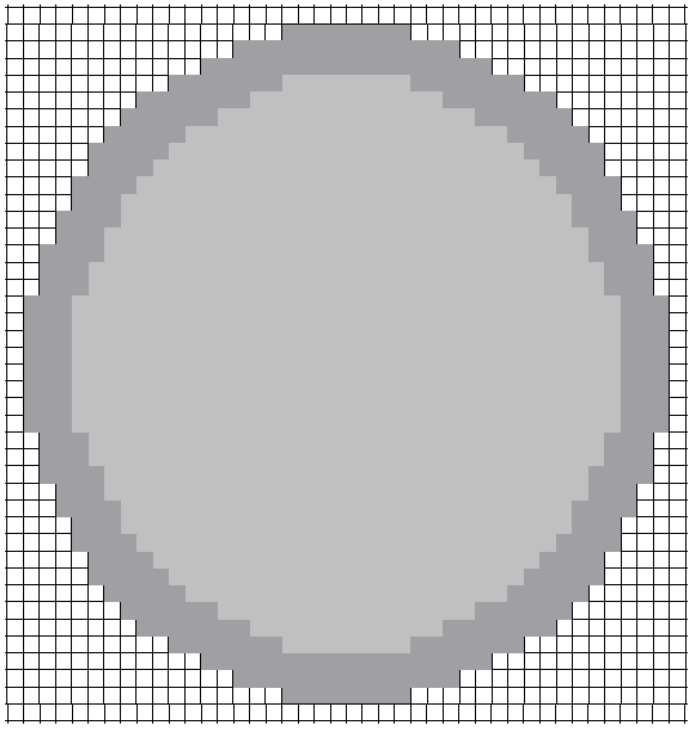

Figure 5. Cross-sectional view of the TORT model of the single pebble cell.

4. RESULTS

Tables 1 through 3 show the results of criticality calculations from TORT, MCNP, and EVENT, using COMBINE-generated cross sections, as well as criticality calculations from EVENT, using

the 75-group and 172-group WIMS master cross section libraries. The continuous-energy MCNP benchmark is also shown. Continuous-energy MCNP results at operating temperature are not shown because continuous-energy cross sections at operating temperature were not available.

As expected, there is excellent agreement between the TORT (S-4 and S-8 approximations), MCNP, and EVENT using the same COMBINE multigroup cross sections, as can be seen from Table 4. In Table 3, the results using the WIMS cross sections in EVENT show very close agreement between the 75-group and 172-group energy structures, indicating that the 75-group energy structure is acceptable.

The difference in k_∞ between TORT and MCNP/COMBINE is 0.037% (within 2 standard deviations of MCNP uncertainty) for S-4 and 0.010% (within 1 standard deviation) for S-8, at operating temperature. The difference between EVENT/COMBINE and MCNP/COMBINE is 0.043% at operating temperature, and 0.035% at cold temperature, (both within 2 standard deviations of MCNP uncertainty). These excellent agreements are expected since all three codes use the same multigroup cross section library. That is, the agreement with MCNP verifies the sufficiency of the geometric models in TORT and EVENT. The TORT and MCNP difference is based on using the P-0 (isotropic) scattering kernel. It was found that including the linearly anisotropic scattering term has negligible effect on k_∞. This was verified with both TORT (S-4) and EVENT.

We used EVENT to compare/evaluate the cross section processing codes against the continuous-energy MCNP. The results of this comparison are shown in Table 5. When compared to the MCNP continuous-energy result, the EVENT results using COMBINE cross sections show a difference of 4.62% for the infinite multiplication factor. This difference is believed to be the result of the way the resonances are treated in COMBINE. Unlike WIMS, COMBINE treats the resonances only in the fast group module, not in the thermal calculation. At the same time, upscattering is only allowed in the thermal calculation. This may be acceptable for light water reactor cell configurations, but in gas cooled reactors a significant fraction of thermal neutrons are scattered up to higher thermal and lower epithermal energies in which a number of resonances occur. Because COMBINE requires the user to fix the fast-thermal boundary at some energy, one can only model accurately either upscattering or resonances, but not both. The EVENT/WIMS' k_∞ differs from the continuous-energy MCNP by 1.84% for the 75-group and 1.79% for the 172-group. Both the COMBINE and WIMS cross sections are outside of 3 standard deviations of the MCNP continuous-energy result. A possible explanation of the differences between the results produced by COMBINE and WIMS and those produced by the continuous-energy MCNP might be the fact that the COMBINE and WIMS codes were intended for application to light-water reactors, which have a different flux spectrum than do graphite-moderated reactors. Also, some of the difference might be attributed to the difference in the point data library (JEF2.2 for WIMS as opposed to ENDF/B-V for MCNP).

The homogenized two-group reaction rates based on EVENT/COMBINE and MCNP using COMBINE and continuous energy cross sections are shown in Table 6. The reaction rates shown

are the fission rate and absorption rate each divided by the total reaction rate. They are homogenized throughout the core, shell, and gas regions, as well as the entire cell, and are divided into two separate groups and a total over all groups. Table 7 compares the reaction rate calculations from EVENT against MCNP. Although there is very good agreement between EVENT and MCNP when they both use the 75-group COMBINE cross sections, there are significant differences between the EVENT/COMBINE and MCNP continuous-energy results, as high as 22% for the fission/total reaction rate for group 1 and 19% for group 2.

The timing study shows that TORT requires much longer computation time than EVENT to achieve comparable accuracy. TORT performs between approximately 4000 and 9000 source, or outer, iterations to converge when performing these calculations, and uses a model containing 74,088 mesh intervals. The EVENT model performs 200 source iterations, and uses a model with 247 hexahedral elements. The computer used for the TORT computations was a Dell Dimension 4100 with a 990 MHz CPU and 512 MB RAM, running Red Hat Linux 7.0. For EVENT computations it was a Dell Precision 330 with a 1.8GHz CPU and 512 MB RAM.

Table 1. Infinite multiplication factors from TORT using COMBINE cross sections at operating temperature.

Order of Scattering	S-2 Quadrature	S-4 Quadrature	S-8 Quadrature
P_0	1.04765	1.04353	1.04381
P_1		1.04353	

Table 2. Infinite multiplication factors from MCNP at cold and operating temperatures using COMBINE and continuous-energy cross sections*.

Temperature	COMBINE 75-Group Cross Sections [a]	Continuous-Energy Cross Sections [b]
Cold	1.12459 ±0.00025	1.17943 ±0.00022
Hot	1.04392 ±0.00024	

* MCNP results used 20 million active particle histories.
[a] COMBINE produced 75-group cross sections based on ENDF/B-V.
[b] Continuous-energy cross sections based on ENDF/B-V.

Table 3. Infinite multiplication factor from EVENT at cold and operating temperatures using COMBINE and WIMS cross sections.

Temperature	COMBINE 75-Group Cross Sections	WIMS 75-Group Cross Sections	WIMS 172-Group Cross Sections
Cold	1.12498	1.20110	1.20050
Hot	1.04347	1.11804	1.11531

Table 4. Percent difference in multiplication factors comparing TORT and EVENT against MCNP/COMBINE [†].

TORT Using COMBINE Cross Sections at Operating Temperature.			
Order of Scattering	S-2	S-4	S-8
P_0	0.36±0.02	-0.04 ±0.02	-0.01 ±0.02
P_1		-0.04 ±0.02	
EVENT Using COMBINE and WIMS Cross Sections			
Temperature	COMBINE 75-Group Cross Sections	WIMS 75-Group Cross Sections	WIMS 172-Group Cross Sections
Cold	0.03 ±0.02	6.80 ±0.02	6.75 ±0.02
Hot	-0.04 ±0.02	7.10 ±0.02	6.84 ±0.02

Table 5. Percent difference in multiplication factors comparing EVENT against MCNP continuous-energy[†].

MCNP Continuous-Energy vs:			
Temperature	EVENT/COMBINE 75-Group Cross Sections	EVENT/WIMS 75-Group Cross Sections	EVENT/WIMS 172-Group Cross Sections
Cold	-4.62 ±0.02	1.84 ±0.02	1.79 ±0.02

Table 6. Homogenized reaction rates at cold temperature in core, shell, and gas regions of the pebble, and the entire cell. Results are from EVENT/COMBINE and MCNP using COMBINE and continuous-energy cross sections [‡].

EVENT/COMBINE		
	Fission/Total	Absorption/Total
Core All Groups	$6.90985\text{X}10^{-3}$	$1.38668\text{X}10^{-2}$
Core Group 1	$1.02782\text{X}10^{-3}$	$1.55665\text{X}10^{-3}$
Core Group 2	$7.18958\text{X}10^{-3}$	$1.44522\text{X}10^{-2}$
Shell All Groups	0.00000	$1.09043\text{X}10^{-4}$
Shell Group 1	0.00000	$3.09760\text{X}10^{-4}$
Shell Group 2	0.00000	$9.95255\text{X}10^{-5}$

[†] The percent difference between an EVENT and MCNP result is[9]:

$diff = 100\left(\frac{E-M}{M}\right)$, with the standard deviation $\sigma_{diff} = \sigma_M\left(100\ \frac{E}{M^2}\right)$.

[‡] The standard deviation for the fission/total reaction rate is $\sigma_{F/T} = \sqrt{\sigma_F^2\left(\frac{1}{T}\right)^2 + \sigma_T^2\left(\frac{F}{T^2}\right)^2}$, and for absorption/total it is $\sigma_{A/T} = \sqrt{\sigma_A^2\left(\frac{1}{T}\right)^2 + \sigma_T^2\left(\frac{A}{T^2}\right)^2}$.

Gas All Groups	0.00000	$3.15381X10^{-2}$
Gas Group 1	0.00000	$6.13643X10^{-2}$
Gas Group 2	0.00000	$3.08819X10^{-2}$
Cell All Groups	$4.05734X10^{-3}$	$8.80113X10^{-3}$
Cell Group 1	$6.10456X10^{-4}$	$1.62223X10^{-3}$
Cell Group 2	$4.21932X10^{-3}$	$9.13848X10^{-3}$
MCNP/COMBINE		
	Fission/Total	Absorption/Total
Core All Groups	$6.96628X10^{-3} \pm 1.56X10^{-6}$	$1.39734X10^{-2} \pm 3.12X10^{-6}$
Core Group 1	$1.02853X10^{-3} \pm 3.71X10^{-7}$	$1.55855X10^{-3} \pm 8.39X10^{-7}$
Core Group 2	$7.25174X10^{-3} \pm 1.62X10^{-6}$	$1.45702X10^{-2} \pm 3.26X10^{-6}$
Shell All Groups	0.00000	$1.08977X10^{-4} \pm 3.45X10^{-8}$
Shell Group 1	0.00000	$3.08387X10^{-4} \pm 6.20X10^{-7}$
Shell Group 2	0.00000	$9.95655X10^{-5} \pm 2.23X10^{-8}$
Gas All Groups	0.00000	$3.15259X10^{-2} \pm 7.05X10^{-6}$
Gas Group 1	0.00000	$6.12631X10^{-2} \pm 2.74X10^{-5}$
Gas Group 2	0.00000	$3.08746X10^{-2} \pm 6.90X10^{-6}$
Cell All Groups	$4.07798X10^{-3} \pm 8.65X10^{-7}$	$8.84207X10^{-3} \pm 1.76X10^{-6}$
Cell Group 1	$6.12742X10^{-4} \pm 2.04X10^{-7}$	$1.62258X10^{-3} \pm 6.17X10^{-7}$
Cell Group 2	$4.24154X10^{-3} \pm 9.00X10^{-7}$	$9.18285X10^{-3} \pm 1.83X10^{-6}$
MCNP Continuous Energy		
	Fission/Total	Absorption/Total
Core All Groups	$8.57311X10^{-3} \pm 4.37X10^{-6}$	$1.63897X10^{-2} \pm 6.76X10^{-6}$
Core Group 1	$1.31046X10^{-3} \pm 1.02X10^{-6}$	$1.94775X10^{-3} \pm 3.08X10^{-6}$
Core Group 2	$8.84314X10^{-3} \pm 4.51X10^{-6}$	$1.69267X10^{-2} \pm 6.98X10^{-6}$
Shell All Groups	0.00000	$1.27747X10^{-4} \pm 1.03X10^{-7}$
Shell Group 1	0.00000	$3.79117X10^{-4} \pm 2.70X10^{-6}$
Shell Group 2	0.00000	$1.18729X10^{-4} \pm 6.05X10^{-8}$
Gas All Groups	0.00000	$3.75157X10^{-2} \pm 2.02X10^{-5}$
Gas Group 1	0.00000	$7.42245X10^{-2} \pm 7.42X10^{-5}$
Gas Group 2	0.00000	$3.68368X10^{-2} \pm 1.98X10^{-5}$
Cell All Groups	$4.38961X10^{-3} \pm 2.22X10^{-6}$	$9.07459X10^{-3} \pm 3.43X10^{-6}$
Cell Group 1	$6.87593X10^{-4} \pm 4.78X10^{-7}$	$1.83816X10^{-3} \pm 2.15X10^{-6}$
Cell Group 2	$4.52380X10^{-3} \pm 2.28X10^{-6}$	$9.33687X10^{-3} \pm 3.54X10^{-6}$

Table 7. Percent difference between EVENT/COMBINE vs. MCNP reaction rates at cold temperature[†].

EVENT/COMBINE vs. MCNP/COMBINE		
	Fission/Total	Absorption/Total
Core All Groups	-0.81 ±0.02	-0.76 ±0.02
Core Group 1	-0.07 ±0.04	-0.12 ±0.05

Core Group 2	-0.86 ±0.02	-0.81 ±0.02
Shell All Groups	NA	0.06 ±0.03
Shell Group 1	NA	0.45 ±0.20
Shell Group 2	NA	-0.04 ±0.02
Gas All Groups	NA	0.04 ±0.02
Gas Group 1	NA	0.17 ±0.04
Gas Group 2	NA	0.02 ±0.02
Cell All Groups	-0.51 ±0.02	-0.46 ±0.02
Cell Group 1	-0.37 ±0.03	-0.02 ±0.04
Cell Group 2	-0.52 ±0.02	-0.48 ±0.02
EVENT/COMBINE vs. MCNP Continuous Energy		
	Fission/Total	Absorption/Total
Core All Groups	-19.40 ±0.04	-15.39 ±0.03
Core Group 1	-21.57 ±0.06	-20.08 ±0.13
Core Group 2	-18.70 ±0.04	-14.62 ±0.04
Shell All Groups	NA	-14.64 ±0.07
Shell Group 1	NA	-18.29 ±0.58
Shell Group 2	NA	-16.17 ±0.04
Gas All Groups	NA	-15.93 ±0.05
Gas Group 1	NA	-17.33 ±0.08
Gas Group 2	NA	-16.17 ±0.05
Cell All Groups	-7.57 ±0.05	-3.01 ±0.04
Cell Group 1	-11.22 ±0.06	-11.75 ±0.10
Cell Group 2	-6.73 ±0.05	-2.12 ±0.04

Table 8. Computation times for TORT [days]

Order of Scattering	S-2	S-4	S-8
P_0	6.4	9.6	11.4
P_1		12.7	

Table 9. Computation times for EVENT [minutes].

Temperature	COMBINE 75-Group Cross Sections	WIMS 75-Group Cross Sections	WIMS 172-Group Cross Sections
Cold	1.0	0.9	5.0
Hot	1.2	1.6	2.6

5. CONCLUSIONS

Comparisons were made among calculations using models of a PBR pebble in a cube of gas coolant using the TORT, EVENT, and MCNP neutron transport codes, and among results obtained using COMBINE, WIMS, and continuous-energy cross sections. The TORT, EVENT, and MCNP models all produce results in the infinite multiplication factor that are in excellent agreement, when using the same COMBINE-produced cross sections, as expected. EVENT has a significant advantage over TORT with respect to model preparation (arbitrary geometry option) and computation time.

When compared to continuous-energy cross sections used in MCNP, the COMBINE-produced cross sections used in EVENT have errors of approximately 5% in k_∞, and those from WIMS have errors of approximately 2%. The COMBINE and WIMS cross sections used in EVENT both produce results that are outside of 3 standard deviations of the MCNP continuous-energy results.

Reaction rates comparing EVENT to MCNP, both using COMBINE 75-group cross sections show excellent agreement as expected, but comparing EVENT/COMBINE to continuous-energy MCNP shows significant differences, some as high as 20%.

Based on criticality calculations, WIMS is more suitable than COMBINE for developing cross sections for PBRs, but its suitability has not yet been fully determined since reaction rate calculations using WIMS cross sections are not available at this time. Also, comparisons must include the hot operating temperature for a thorough evaluation.

6. REFERENCES

1. W. K. Terry, H. D. Gougar, and A. M. Ougouag, “Direct Deterministic Method for Neutronics Analysis and Computation of Asymptotic Burnup Distribution in a Recirculating Pebble-Bed Reactor,” *Annals of Nuclear Energy*, **29** pp. 1345-1364 (2002).
2. Grimesey, R., Nigg, D., and Curtis, R., *COMBINE/PC-A Portable ENDF/B v5 Neutron Spectrum and Cross-Section Generation Program*, INEEL Internal Report EGG-2589, (April 1990).
3. Amouyal, A., Benoist, P. and Horowitz, J., "New Method for Determining the Thermal Utilization Factor in a Unit Cell," *Journal of Nuclear Energy*, **6**, pp. 79-98 (1957).
4. J. Valko, P.V. Tsvetkov, J.E. Hoogenboom, "Calculation of the Dancoff Factor for Pebble Bed Reactors," *Nuclear Science and Engineering*, **135**, 304-307 (2000).
5. WIMS8A User's Guide, ANSWERS/WIMS(99), AEA Technology, (May 1999).

6. Rhoads, W.A. and Simpson, D.B., *The TORT Three-Dimensional Discrete Ordinates Neutron/Photon Transport Code, (TORT Version 3)*, Oak Ridge National Laboratory, (1997).
7. C.R.E. de Oliveira and A.J.H. Goddard, "EVENT - A Multidimensional Finite Element-Spherical Harmonics Radiation Transport Code," *Proceedings of the OECD International Seminar on 3D Deterministic Radiation Transport Codes*, Paris, (December 01-02, 1996).
8. Briesmeister, J.F. (Ed), *MCNP^{TM} -A General Monte Carlo N-Particle Transport Code-Version 4C*, LANL report LA–13709–M, (March 2000).
9. Philip R. Bevington, *Data Reduction and Error Analysis for the Physical Sciences*, McGraw-Hill Book Company, New York, US (1969).